Steel and Composite Structures, Vol. 6, No. 3 (2006) 237-255
DOI: http://dx.doi.org/10.12989/scs.2006.6.3.237

Short- and long-term analyses of composite beams with partial interaction stiffened by a longitudinal plate

Gianluca Ranzi†

School of Civil Engineering, The University of Sydney, NSW 2006, Australia

(Received April 19, 2005, Accepted December 28, 2005)

Abstract. This paper presents a novel analytical formulation for the analysis of composite beams with partial shear interaction stiffened by a bolted longitudinal plate accounting for time effects, such as creep and shrinkage. The model is derived by means of the principle of virtual work using a displacement-based formulation. The particularity of this approach is that the partial interaction behaviour is assumed to exist between the top slab and the joist as well as between the joist and the bolted longitudinal stiffening plate, therefore leading to a three-layered structural representation. For this purpose, a novel finite element is derived and presented. Its accuracy is validated based on short-and long-term analyses for the particular cases of full shear interaction and partial shear interaction of two layers for which solutions in closed form are available in the literature. A parametric study is carried out considering different stiffening arrangements to investigate the influence on the short-and long-term behaviour of the composite beam of the shear connection stiffness between the concrete slab and the steel joist, the stiffness of the plate-to-beam connection, the properties of the longitudinal plate and the concrete properties. The values of the deflection obtained from the finite element simulations are compared against those calculated using the effective flexural rigidity in accordance with EC5 guidelines for the behaviour of elastic multi-layered beams with flexible connection and it is shown how the latter well predicts the structural response. The proposed numerical examples highlight the ease of use of the proposed approach in determining the effectiveness of different retrofitting solutions at service conditions.

Keywords: composite beams; finite element method; partial interaction; stiffening; time effects.

1. Introduction

In the second half of the last century, there has been an increasing trend towards the use and development of composite materials which, combining the advantageous mechanical and structural properties of different materials, lead to composite enhanced characteristics. In the field of civil engineering, one of the most significant contributions in this sense is certainly the one of composite steel-concrete construction. Despite its first applications are dated back to 1894, (Cosenza and Zandonini 1999) there is still an ongoing intense research activity related to this form of construction.

In the case of composite beams, the interaction between the reinforced concrete slab and the steel joist is provided by means of shear connectors (Oehlers and Bradford 1995). Already in the late 40's and 50's, it was highlighted that their high deformability needed to be accounted for to provide an adequate modelling of the composite response, i.e., partial interaction behaviour; among these first

†Lecturer, E-mail: G.Ranzi@civil.usyd.edu.au

studies, the one by Newmark *et al.* (1951) is one of the most cited papers in this area and, due to its popularity, their analytical formulation is usually simply referred to in literature as Newmark model. Since then several studies have focussed on the behaviour of composite steel-concrete beams (two-layered members) in the linear-elastic range (Ranzi *et al.* 2004, Seracino *et al.* 2004, Faella *et al.* 2002, Wu *et al.* 2002, Cosenza and Mazzolani 1993), in the nonlinear range (Čas *et al.* 2004, Dall'Asta and Zona 2004, Loh *et al.* 2004, Faella *et al.* 2003, Ayoub 2001, Salari and Spacone 2001, Ayoub and Filippou 2000, Fabbrocino *et al.* 2000, Gattesco 1999, Nguyen *et al.* 1998, Oehlers and Sved 1995), accounting for time effects (Virtuoso and Vieira 2004, Fragiacomo *et al.* 2002, Kwak and Seo 2002, Dezi *et al.* 1998, 1996, Gilbert and Bradford 1995) and including shear-lag effects (Amadio and Fragiacomo 2002, Dezi *et al.* 2001). Nevertheless, it is outside the scope of the present paper to provide an extensive literature review.

Goodman and Popov (1968) further extended Newmark model to account for composite beams formed of three layers accounting for the deformability of the shear connection between adjacent layers. They considered equal and rectangular cross-sections and applied their formulation to the instantaneous analysis of determinate structures, in particular of simply supported three-layered wood beams subjected to a point load applied at mid-span and to two point loads applied at third points.

This paper proposes a novel analytical model for the analysis of three-layered composite beams with partial shear interaction accounting for time effects, such as creep and shrinkage, and the analytical representation is derived for the particular case of a composite beam stiffened by a longitudinal plate in which the partial interaction occurs between the slab and the steel joist as well as between the joist and the stiffening plate. The formulation is derived by means of the principle of virtual work in which the problem is expressed using a specified displacement field.

Based on this proposed model, a novel 13*dof* finite element is derived. Its nodal freedoms include the axial displacements of each layer, the vertical displacements and the rotations at the ends of the element. The accuracy of this modelling technique is assessed for both short-and long-term analyses against solutions available in closed form for the cases in which both shear connection stiffnesses tend to infinity (Gere 2001, Ranzi and Bradford 2005), and where only one connection stiffness is infinitely high, thus degenerating into the conventional two-layered composite with partial interaction (Ranzi and Bradford 2006).

A parametric study is then presented which considers different stiffening arrangements and highlights the influence on the short-and long-term behaviour of the composite beam of the shear connection stiffness between the concrete slab and the steel joist, the stiffness of the plate-to-beam connection, the properties of the longitudinal plate and the concrete properties. The values of the deflection obtained from the finite element simulations are compared against those calculated using the effective flexural rigidity based on the EC5 guidelines provided in Annex B for the behaviour of elastic multi-layered beams with flexible connection (EC5 1995).

2. Basic assumptions

A prismatic beam formed by three layers (here representing a steel-concrete composite beam stiffened by a longitudinal plate) is considered and shown in Fig. 1. In its undeformed state, it occupies the cylindrical region $V=A\times[0, L]$ generated by translating its cross-section A, with regular boundary ΩA, along a rectilinear axis orthogonal to the cross-section, and assumed to be parallel to the Z axis of the ortho-normal reference system $\{O; X, Y, Z\}$. For generality, the

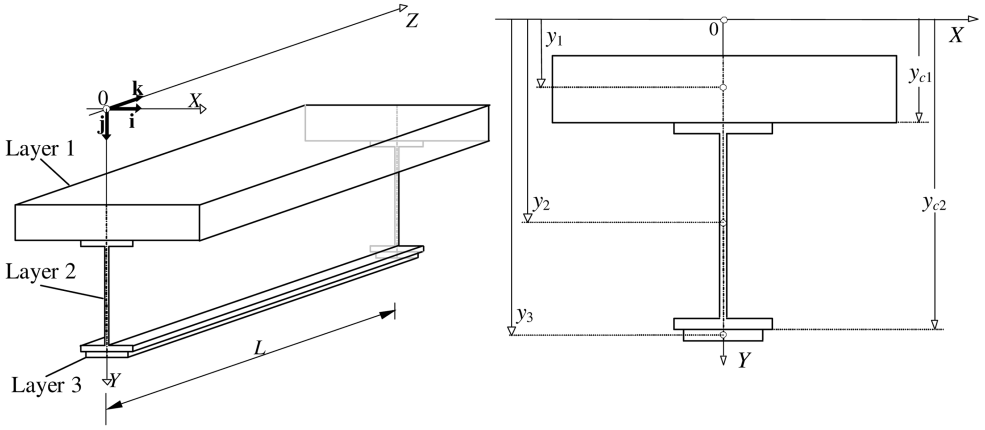

Fig. 1 Typical composite beam and cross-section

formulations are derived for a beam segment of length L and about an arbitrary coordinate system as shown in Fig. 1.

The composite cross-section A is assumed symmetric about the plane of bending, the coordinate plane YZ being taken as the plane of symmetry. For the composite cross-section considered, $A1$ consists of the reinforced slab, further sub-divided into A_c and A_r, the concrete component and the reinforcement respectively, $A1 = A_c \cup A_r$; A_2 represents the cross-section of the steel joist and it is denoted as A_b; while A_3 represents the cross-section of the longitudinal steel plate referred to as A_p.

It is assumed that Euler-Bernoulli beam theory applies to all three layers and therefore plane sections are assumed to remain plane except for discontinuities at the connection interfaces.

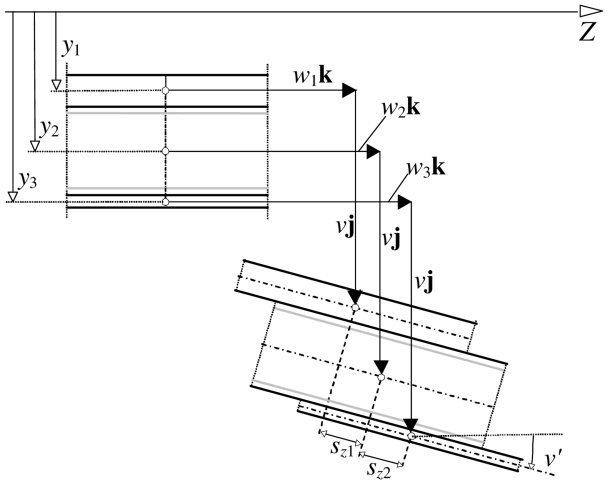

Fig. 2 Displacement field

3. Kinematic model

The position of a generic material point P can be expressed in the undeformed state of the beam by the vector $\mathbf{p}$ as

$$\mathbf{p} = P - O = x\mathbf{i} + y\mathbf{j} + z\mathbf{k} \qquad \forall (x, y) \in A, z \in [0, L] \tag{1}$$

in which $\mathbf{i},\mathbf{j},\mathbf{k}$ represent the unit vectors parallel to the axes of the adopted ortho-normal reference system $\{O; X, Y, Z\}$. The composite action is provided by the two shear connections assumed to be uniformly distributed along rectilinear lines at the interfaces between the three layers, whose domains consist of $(x, y) = (0, y_{c1})$ and $(x, y) = (0, y_{c2})$, with $z \in [0, L]$; y_{c1} and y_{c2} are defined in Fig. 1 and denote the locations of the two interfaces. These shear connections allow relative displacements to occur in the longitudinal direction between adjacent layers usually referred to as slip.

The kinematic behaviour of the composite beam is expressed in terms of $w_1(z; t)$, $w_2(z; t)$, $w_3(z; t)$ and $v(z; t)$ which are the axial displacements of the three layers and the vertical deflection respectively as shown in Fig. 2. Therefore, the adopted displacement field can be expressed as $\mathbf{d}(z; t) = [w_1(z; t), w_2(z; t), w_3(z; t), v(z; t)]^T$. Differentiating the deflection v with respect to the coordinate z along the beam length yields the expressions for the rotation $\theta (= -v')$ and curvature $\kappa (= -v'')$, in which the prime represents a derivative with respect to z.

The admissible displacement of a generic point in the composite beam is shown in Fig. 2 and defined by vector $\mathbf{r}(x, y, z; t)$ as (with $i = 1, 2, 3$)

$$\mathbf{r}(x, y, z; t) = v(z; t)\mathbf{j} + [w_i(z; t) - (y - y_i)v'(z; t)]\mathbf{k} \qquad \forall (x, y) \in A_i, z \in [0, L] \tag{2}$$

The vectors expressing the slips at the interfaces between the top two layers and the remaining two respectively are defined as

$$\mathbf{s_1}(z;t) = \mathbf{s}_{z1}(z;t)\mathbf{k} = [w_2(z;t) - w_1(z;t) + h_1 v'(z;t)]\mathbf{k} \tag{3a}$$

$$\mathbf{s_2}(z;t) = \mathbf{s}_{z2}(z;t)\mathbf{k} = [w_3(z;t) - w_2(z;t) + h_2 v'(z;t)]\mathbf{k} \tag{3b}$$

in which s_{z1} and s_{z2} are the slips at the interface between layers 1 and 2 and between 2 and 3 respectively, $h_1 = y_2 - y_1$ and $h_2 = y_3 - y_2$.

The only non-vanishing strain components of the partial interaction problem is ε_z which is defined as (with $i = 1, 2, 3$)

$$\varepsilon_z = \frac{\partial \mathbf{r} \cdot \mathbf{k}}{\partial z} = \varepsilon_{zi}(z;t) = w_i'(z;t) - (y - y_i)v''(z;t) \qquad \forall (x, y) \in A_i, z \in [0, L] \tag{4}$$

4. Material properties

The time-dependent behaviour of the concrete is modeled accounting for creep and shrinkage effects based on the integral-type creep law (CEB 1984) as

$$\varepsilon_{tot}(t) - \varepsilon_{sh}(t) = \sigma_c(t_0)J(t, t_0) + \int_{t_0^+}^{t} J(t, \tau)d\sigma_c(\tau) \tag{5}$$

where t is the time from casting of the concrete (equal to t_k), t_0 is the time of first loading, time t is subdivided by discrete times t_0, t_1, t_2, ... t_i, ... t_k, $\sigma_c(t_i)$ (also referred to as σ_{ci}) is the concrete stress calculated at time t_i, $\varepsilon_{tot}(t)$ is the total axial strain which combines both stress-dependent and stress-independent strains, $\varepsilon_{sh}(t)$ is the shrinkage strain (while other stress-independent strains, e.g. thermal dilatation, could be modelled in a similar manner), and $J(t, \tau)$ is the creep function defined as the strain at time t due to a constant unit stress acting from time τ to time t. The superposition integral of Eq. (5) is here approximated by means of the step-by-step procedure, applying the trapezoidal rule; (CEB 1984) this approximation implies that: (Moin 2001)

$$\int_{t_0^+}^{t} J(t, \tau)\,\mathrm{d}\sigma_c(\tau) \cong \sum_{i=1}^{k} \frac{1}{2}[J(t_k, t_i) + J(t_k, t_{i-1})][\sigma_c(t_i) - \sigma_c(t_{i-1})] \tag{6}$$

and substituting Eq. (6) into Eq. (5) yields

$$\varepsilon_{ck} - \varepsilon_{shk} \cong \sigma_c(t_0)J(t_k, t_0) + \sum_{i=1}^{k} \frac{1}{2}[J(t_k, t_i) + J(t_k, t_{i-1})][\sigma_c(t_i) - \sigma_c(t_{i-1})] \tag{7}$$

where ε_{ck} is the total axial strain which combines both stress-dependent and stress-independent strains, ε_{shk} is the shrinkage strain, and $J(t_k, t_i)$ is the creep function which is defined as the strain at time t_k caused by a constant unit stress acting from time t_i to time t_k.

It is also assumed that the time-dependent behaviour of the concrete is described by Eq. (7) in both compression and tension. This is acceptable for stress levels in compression less than about one half of the compressive strength of the concrete, and for tensile stresses less than about one half of the tensile strength of the concrete, as recommended by Gilbert (1988) and Bažant and Oh (1984); and so the results obtained using the proposed approach are assumed to be acceptable from a qualitative and quantitative viewpoint when the calculated stresses remain in this stress range. Nevertheless, when the calculated stresses are outside this range the results might still be meaningful from a qualitative viewpoint, for example in comparing the effects of different cross-sectional properties, while other nonlinearities, i.e., concrete cracking, might need to be accounted for to yield quantitatively acceptable results.

It is assumed that the reinforcing bars, the steel joist and the additional longitudinal plate behave in a linear-elastic fashion, and E_r, E_s and E_p are the relevant elastic moduli for the reinforcement, steel joist and longitudinal plate respectively.

It is also assumed that both shear connections, i.e., the one between the reinforced concrete slab and the steel joist and the one between the joist and the additional longitudinal plate, are uniformly spread at the interfaces between adjacent layers and behave in a linear-elastic fashion; their constitutive relationships can be expressed as

$$g_{z1}(z;t) = k_{z1}s_{z1}(z;t) = k_{z1}[w_2(z;t) - w_1(z;t) + h_1 v'(z;t)] \tag{8a}$$

$$g_{z2}(z;t) = k_{z2}s_{z2}(z;t) = k_{z2}[w_3(z;t) - w_2(z;t) + h_2 v'(z;t)] \tag{8b}$$

in which the connection stiffness $k_{z1}(k_{z2})$ relates the longitudinal force per unit length $g_{z1}(g_{z2})$ to the corresponding slip $s_{z1}(s_{z2})$.

5. Global equilibrium condition

The principle of virtual work is applied to obtain the weak formulation of the partial interaction problem for each kinematically admissible virtual displacement as

$$\sum_{i=1}^{3}\int_{L}\int_{A_i}\sigma_{zi}\hat{\varepsilon}_{zi}\mathrm{d}a\mathrm{d}z+\sum_{j=1}^{2}\int_{L}g_{zj}\hat{s}_{zj}\mathrm{d}z=\sum_{i=1}^{3}\int_{L}\int_{A_i}\mathbf{b}\cdot\hat{\mathbf{r}}\mathrm{d}a\mathrm{d}z+\sum_{i=1}^{3}\int_{L}\int_{\Omega A_i}\mathbf{q}\cdot\hat{\mathbf{r}}\mathrm{d}l\mathrm{d}z+\sum_{i=1}^{3}\int_{A_{i0,L}}\mathbf{q}\cdot\hat{\mathbf{r}}\mathrm{d}a\quad\forall\hat{\mathbf{r}}\tag{9}$$

in which $i = 1, 2, 3$ represent the three layers, $j = 1, 2$ denote the two interface connections, ΩA_i represents the contour of the domain A_i, σ_{zi} represents those stresses which produce internal work, i.e., active stresses, g_{zj} is the shear flow which occurs at the j-th connection interface, and the third integral on the right hand-side of the equation represents the work done by the surface forces applied at the cross-section at the ends of the beam segment considered. Virtual displacements and strains have been identified by means of a hat "^" placed above the variable considered.

The solution of the problem is then sought at each time step in the spaces of the regular functions fulfilling the kinematic boundary conditions.

For generality, both quasi-static body and surface forces have been considered. These have been referred to as **b** and **q** respectively and have been collected in the following vectors as

$$\mathbf{f}=\begin{bmatrix}\int_{A_1}\mathbf{b}\cdot\mathbf{k}\mathrm{d}a+\int_{\Omega A_1}\mathbf{q}\cdot\mathbf{k}\mathrm{d}l\\ \int_{A_2}\mathbf{b}\cdot\mathbf{k}\mathrm{d}a+\int_{\Omega A_2}\mathbf{q}\cdot\mathbf{k}\mathrm{d}l\\ \int_{A_3}\mathbf{b}\cdot\mathbf{k}\mathrm{d}a+\int_{\Omega A_3}\mathbf{q}\cdot\mathbf{k}\mathrm{d}l\\ \int_{A}\mathbf{b}\cdot\mathbf{j}\mathrm{d}a+\int_{\Omega A}\mathbf{q}\cdot\mathbf{j}\mathrm{d}l\\ \sum_{i=1}^{3}\int_{A_i}(y-y_i)\mathbf{b}\cdot\mathbf{k}\mathrm{d}a+\sum_{i=1}^{3}\int_{\Omega A_i}(y-y_i)\mathbf{b}\cdot\mathbf{k}\mathrm{d}l\end{bmatrix};\ \mathbf{Q}_{0,L}=\begin{bmatrix}\int_{A_1}\mathbf{q}\cdot\mathbf{k}\mathrm{d}a\\ \int_{A_2}\mathbf{q}\cdot\mathbf{k}\mathrm{d}a\\ \int_{A_3}\mathbf{q}\cdot\mathbf{k}\mathrm{d}a\\ \int_{A_{0,L}}\mathbf{q}\cdot\mathbf{j}\mathrm{d}a\\ \sum_{i=1}^{3}\int_{A_i}(y-y_i)\mathbf{q}\cdot\mathbf{k}\mathrm{d}a\end{bmatrix}_{0,L}\tag{10a,b}$$

where **f**, $\mathbf{Q_0}$ and $\mathbf{Q_L}$ represent the vectors of actions applied at time t_k along the beam and at the cross-sections at the ends of the beam segment considered, i.e., at $z = 0, L$.

The time-dependent behaviour of the concrete at time t_k requires the stresses resisted by the concrete at time t_i ($i = 0, ..., k$-1) to be accounted for as defined in Eq. (7). This is accomplished by recording the concrete stress resultants at time t_k as follows

$$\mathbf{f}_c=\left[\int_{A_c}\sum_{i=0}^{k-1}\sigma_{zci}\Delta_{2ki}\mathrm{d}a\quad 0\quad 0\quad 0\quad 0\quad 0\quad\int_{A_c}\sum_{i=0}^{k-1}(y-y_1)\sigma_{zci}\Delta_{2ki}\mathrm{d}a\quad 0\right]\tag{11}$$

in which σ_{zci} is the longitudinal active stress resisted by the concrete at time t_i and Δ_{2ki} is defined in appendix.

Taking account of the constitutive relationships, Eq. (9) can be re-written to highlight the different variables of the problem in the following compact form

$$\int_L \{[T\mathscr{A}\mathbf{d} + \mathbf{f}_c - \mathbf{f}_{sh}] \cdot \mathscr{A}\hat{\mathbf{d}}\}\mathrm{d}z = \int_L (\mathbf{f} \cdot \mathscr{B}\hat{\mathbf{d}})\mathrm{d}z + [\mathbf{Q} \cdot \mathscr{B}\hat{\mathbf{d}}]_{0,L} \qquad \forall \hat{\mathbf{d}} \tag{12}$$

in which $\mathbf{f_{sh}}$ is the vector related to the shrinkage strain ε_{shk} at time t_k defined as

$$\mathbf{f}_{\mathbf{sh}}^{\mathbf{T}} = \Delta_{1k}\varepsilon_{shk}\left[\int_{A_c}\mathrm{d}a \quad 0 \quad 0 \quad 0 \quad 0 \quad 0 \quad \int_{A_c}(y - y_1)\mathrm{d}a \quad 0\right] \tag{13}$$

and the stiffness transformation matrix **T**, the formal differential operators $\mathscr{A}$ and $\mathscr{B}$ and the relevant cross-sectional and material properties are defined in appendix and are calculated at each time step accounting for the time-dependent behaviour of the concrete.

The step-by-step procedure requires several analyses to be carried out to complete the time analysis, each relying on the results of the previous analyses as described by Eq. (7) and recalculating $\mathbf{f_c}$ based on Eq. (11).

6. Finite element formulation

A novel finite element is derived to model the partial interaction behaviour of a three-layered beam whose freedoms are depicted in Fig. 3 and include the axial displacements of the three layers observed at the levels y_i (with i = 1, 2, 3), vertical displacements and rotations at both element ends. The shape functions adopted for the 13*dof* proposed element include a cubic function to approximate the vertical displacement and parabolic functions for the axial displacements of the layers; internal nodes related to the axial displacements have been introduced to achieve these polynomials. This element includes the minimum number of freedoms to provide a robust and stable element which does not suffer from curvature locking problems. Mathematically, the adopted displacement field **d** is then approximated by $\mathbf{N_e}\,\mathbf{d_e}$, where $\mathbf{d_e}$ is the vector of the nodal displacements (Fig. 3) and $\mathbf{N_e}$ is the interpolation matrix collecting the relevant shape functions. The finite element is then derived based on the weak formulation expressed by Eq. (12) adopting the approximated displacement field as

$$\int_L \{(\mathscr{A}\mathbf{N_e})^T[\mathbf{T}(\mathscr{A}\mathbf{N_e})\mathbf{d_e} + \mathbf{f}_c - \mathbf{f_{sh}}] \cdot \hat{\mathbf{d}}_\mathbf{e}\}\mathrm{d}z = \int_L \left[(\mathscr{B}\mathbf{N_e})^T\mathbf{f}\right] \cdot \hat{\mathbf{d}}_\mathbf{e}\mathrm{d}z + \left[(\mathscr{B}\mathbf{N_e})^T\mathbf{Q}\right]_{0,L} \cdot \hat{\mathbf{d}}_{e0,L} \tag{14}$$

where all notation is defined in appendix. Conventional finite element procedures are then utilized to assemble the vectors and matrices for the whole structure and to perform the structural analysis. (Cook *et al.* 2001).

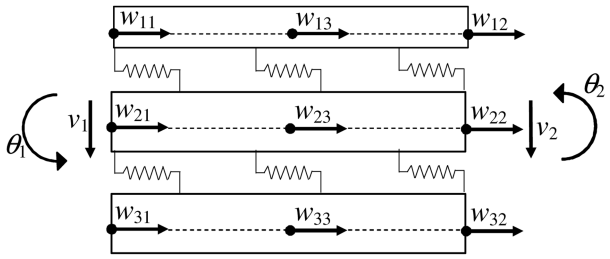

Fig. 3 Freedoms of the proposed three-layered 13*dof* finite element

7. Validation against closed form solutions

The accuracy of the proposed 13*dof* element depicted in Fig. 3 is validated against solutions available in closed form for the extreme cases in which firstly both shear connection stiffnesses tend to infinity (full shear interaction, FSI) using the expressions presented by Gere (2001) for the short-term analysis and those by Ranzi and Bradford (2005) for the long-term one and, secondly, for the short-and long-term analyses where only one infinitively rigid shear connection exists, degenerating into the case of partial shear interaction (PSI) of two-layered beams (Ranzi and Bradford 2006). These solutions approximate the concrete time-dependent behaviour expressed by the superposition integral of equation (5) by means of the algebraic methods, such as the age-adjusted effective modulus method (AEMM), the mean stress method (MS) and the effective modulus method (EM) (CEB 1984, Bažant 1972).

The comparisons have been carried out based on the composite cross-section already extensively used in literature and first proposed by Tarantino and Dezi (1992) which is formed by a rectangular slab (2300 mm × 200 mm), a fabricated steel joist with top flange 300 mm × 20 mm, web 1550 mm × 15 mm, bottom flange 450 mm × 30 mm. For the validation process, the bottom flange of the specified steel joist was "shared" in the three-layered representation between the bottom flange of the steel joist (i.e., layer 2) and the additional plate (i.e., layer 3) while adopting an infinite stiff shear connection between the two. The elastic modulus adopted for the reinforcement, joist and longitudinal plate was 210 000 MPa and the one for the concrete was 34 219 MPa. For the long-term analysis a creep coefficient of 2 and a shrinkage deformation of 200×10^{-6} were specified. The creep effects due to external loads have been modeled by means of the AEMM method while shrinkage effects have been calculated using the MS method as recommended by Dezi *et al.* (1996, 1998); for this reason, aging coefficients of 0.8 and 0.5 have been utlised in the modeling of external loads and of shrinkage effects respectively. The AEMM and MS methods require two analyses to fully complete the time-dependent analysis, which are an instantaneous analysis (i.e., at time t_0, where t_0 is defined as the time of first loading) and an analysis that is performed at one step in time (at the prescribed time t). The applicability of these models to describe the concrete behaviour is affected by the same limitations (i.e., related to cracking and other nonlinearities) already outlined for the step-by-step procedure.

For clarity, two dimensionless stiffness parameters $\gamma_j L$ (j = 1, 2) are introduced to better describe the rigidity of the two shear connections; these are equivalent to the dimensionless αL coefficient identified by Girhammar and Pan (1993) for the case of two-layered beams. The proposed $\gamma_j L$ (j = 1, 2) parameters are defined as

$$\gamma_j = \left[k_j \left(\frac{1}{\tilde{A E}_j} + \frac{1}{\tilde{A E}_{j+1}} + \frac{h_j^2}{\tilde{I E}_j + \tilde{I E}_{j+1}} \right) \right]^{\frac{1}{2}} \tag{15}$$

The validation has been carried out for the case of a 25 m simply supported beam subjected to a uniformly distributed load of 64.56 kN/m and, for clarity, the results from the instantaneous analysis, the ones due to creep and the ones accounting for shrinkage effects have been presented separately.

The results obtained for the full interaction analysis using the proposed modeling technique with $\gamma_1 L \to \infty$ and $\gamma_2 L \to \infty$ (i.e., infinitely rigid shear connection) and those from the closed form solutions

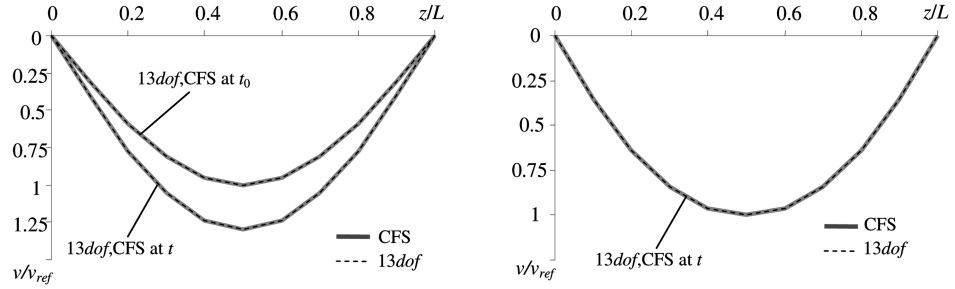

(a) Short-term and long-term (due to creep) values (b) Long-term values (due to shrinkage)

Fig. 4 Short-term and long-term deflection of a simply supported beam subjected to a uniformly distributed load for $\gamma_1 L \to \infty$ and $\gamma_1 L \to \infty$ (Full shear interaction)

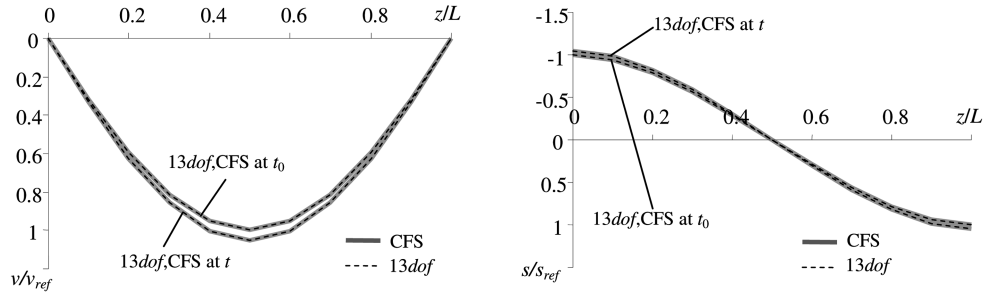

(a) Deflection (b) Slip between layers 1 and 2

Short- and long-term analyses (accounting for creep effects only)

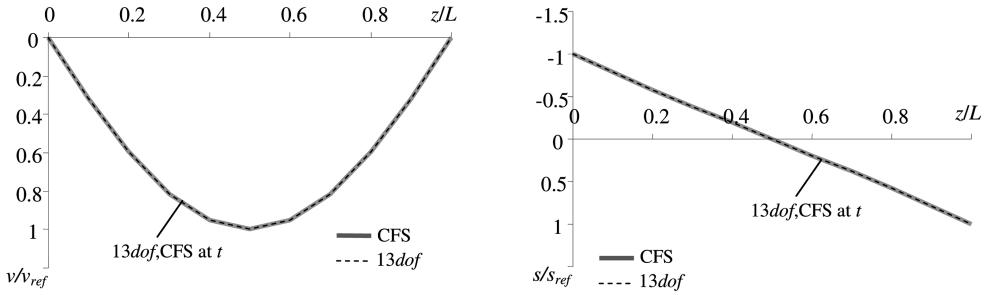

(c) Deflection (d) Slip between layers 1 and 2

Fig. 5 Short-term and long-term analyses of a simply supported beam subjected to a uniformly distributed load for $\gamma_1 L = 1$ and $\gamma_2 L \to \infty$ (Partial shear interaction of conventional 2-layered beam)

are shown in Fig. 4 to perfectly match. Similar agreement with the solutions available in closed form has been noted for the partial interaction analysis of a two-layered beam modeled using the proposed formulation with $\gamma_1 L \to 1$ and $\gamma_2 L \to \infty$ as depicted in Fig. 5. The plotted variables have been non-dimensionalised for clarity; in particular, for the case of the deflection, all values have been non-dimentionalised against the short-term values calculated at mid-span, while for the slip the short-term values at the roller support have been used as reference.

8. Parametric study

A parametric investigation has been carried out by means of the proposed 13*dof* element (Fig. 3) on a case study for which different retrofitting solutions have been considered based on the beam layout and cross-sectional properties introduced for the validation process.

The influence of the shear connection stiffness between the concrete slab and the steel joist, the stiffness of the plate-to-beam connection, the properties of the longitudinal plate and the concrete properties on the short-and long-term behaviour of the composite beam has been investigated; for clarity, creep and shrinkage effects have been considered separately. Four different stiffening arrangements have been considered which include: (i) no additional longitudinal plate (this arrangement has been referred to Arrangement 1 or simply A1); (ii) the longitudinal plate extends over the middle quarter span of the beam (referred to as A2); (ii) the longitudinal plate is placed over the middle half of the

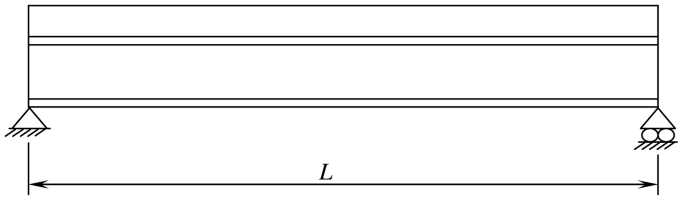

(a) No longitudinal plate – Arrangement A1

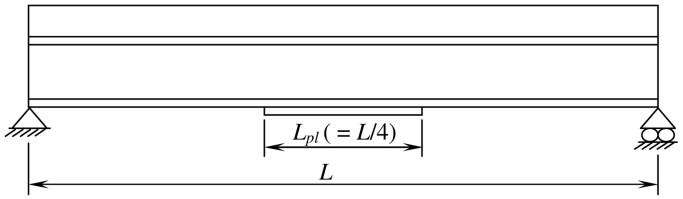

(b) Longitudinal plate over the middle quarter of the span – Arrangement A2

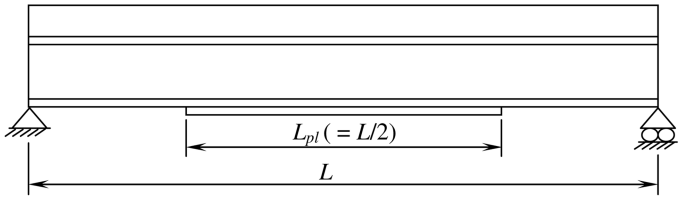

(c) Longitudinal plate over the middle half of the span – Arrangement A3

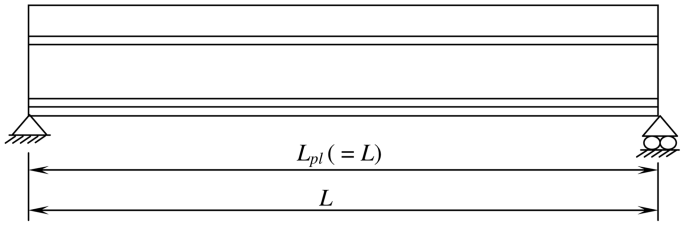

(d) Longitudinal plate over the whole span – Arrangement A4

Fig. 6 Stiffening arrangements considered in the parametric study

Table 1 Stiffness values for the two shear connections $\gamma_j L$ (j = 1, 2)

$\gamma_1 L$	k_1(kN/m^2)	$\gamma_2 L$	k_2(kN/m^2)
100	32681684.72	100	34377206.84
1	3268.16	10	343772.06
		1	3437.72
		0.1	34.37

beam (referred to as A3); (iv) the longitudinal plate spans over the full length of the beam (referred to as A4). For clarity, these arrangements are illustrated in Fig. 6.

The time-dependent behaviour of the concrete has been modelled by means of the step-by-step procedure subdividing the time domain into 80 intervals. The age of concrete at the beginning of shrinkage has been taken as 4 days and the external uniformly distributed load has been assumed to be applied at 28 days. All material properties have been calculated in accordance with guidelines (CEB-FIB 1993); for this purpose, a relative humidity (RH) of the environment of 80%, a concrete strength of 32 MPa, the use of normal and rapid hardening cements N and R, i.e., s = 0.25, have been adopted unless noted otherwise. (CEB-FIB 1993) Regarding the cross-sectional properties, a 450 mm × 50 mm longitudinal plate has been specified for the different stiffening arrangements unless noted otherwise and, recalling the constitutive model introduced for the shear connection in Eqs. (8), several combinations of their stiffnesses have been considered; nevertheless, in the following only the most significant results are presented and these relate to the shear connection stiffnesses outlined in Table 1.

8.1. Effects of the stiffnesses of the two interface shear connections

The four arrangements (Fig. 6) considered in this parametric study lead to different structural responses depending on the combinations of stiffnesses adopted for the shear connection. Figs. 7 and 8 depict the variation of the mid-span deflection and the slip at the bottom shear connection calculated at the extremes of the longitudinal plate; therefore, depending on the arrangement considered, the latter slip is calculated at different locations.

Fig. 7 highlights how for higher stiffness values of the bottom shear connection the short-term deflection can decrease up to approx. 30% (Fig. 7(b)) when compared against the unstiffened solution, while the top shear connection stiffness can reduce the deflection more than 40% (Fig. 7(a)). Creep effects tend to slightly reduce the influence of the top shear connection while no significant change is noted in time for the bottom shear connection. As expected, stiffer shear connection rigidities between the slab and the steel joist produce greater shrinkage loading and, also in this case, the rigidity of the bottom shear connection plays an important role in the overall behaviour.

In general, the end slip of the top shear connection, i.e., s_{z1}, is mainly affected by the rigidity of the top interface, except for low values of $\gamma_1 L$ where both $\gamma_2 L$ and the type of stiffening arrangement adopted affect the top slip values with variations of the order of 10%; similar behaviour has been noted also for the long-term analyses.

The slip calculated at the plate-to-beam connection is primarily affected by its rigidity and by the stiffening arrangement considered. For all arrangements, the slip calculated at the extreme of the longitudinal plate tends to decrease while increasing $\gamma_2 L$; it is worth noting that for arrangement A4, the values of the slip calculated at the support (i.e., the stiffening occurs throughout the beam length) are greater than those determined for the other two arrangements, i.e., A2 and A3, at high values of $\gamma_2 L$,

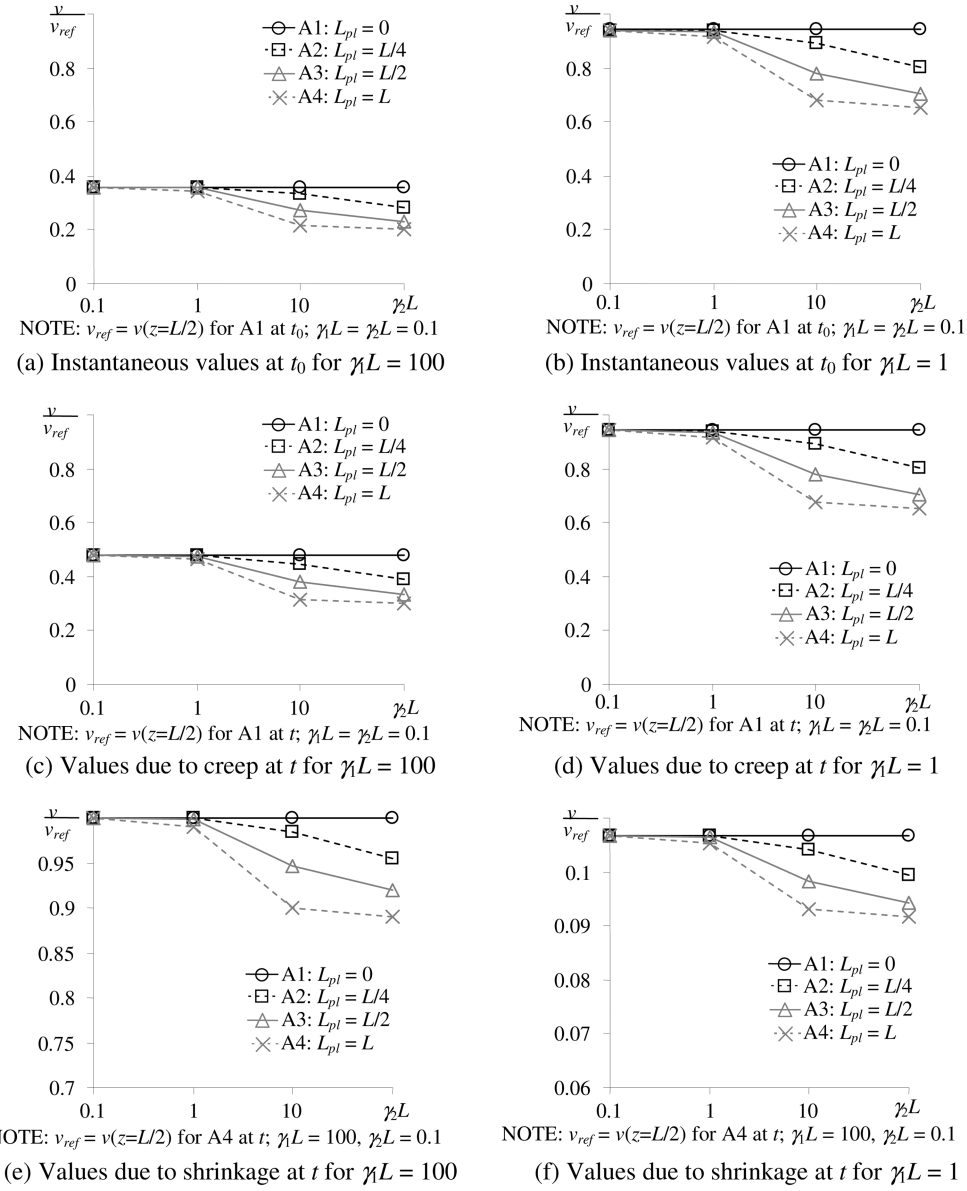

Fig. 7 Deflection at mid-span

while this trend is inverted for low $\gamma_2 L$ values as shown in Fig. 8. As the short-and long-term (due to creep) slip values were observed to follow a very similar trend, only the long-term results have been reported.

8.2. Effects of dimensions of the additional longitudinal plate

The size of the plate significantly affects the overall response as outlined in Table 2 which illustrate the increase of the mid-span deflection and of the bottom slip calculated at the extreme of the additional

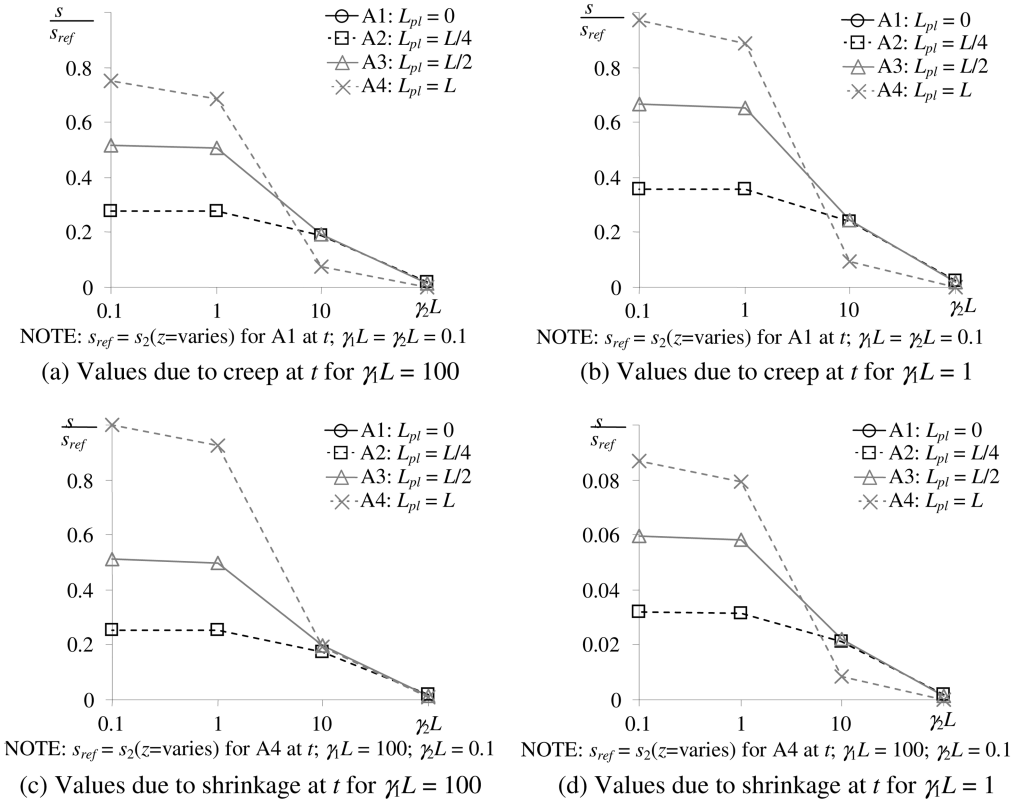

Fig. 8 Slip at the interface between the steel joist and the longitudinal plate. Values calculated at the extremes of the longitudinal plate

longitudinal plate when reducing the thickness of the bottom plate (i.e., layer 3) from 50 mm (considered in Figs. 7 and 8) to 10 mm.

Higher mid-span deflections are obtained while increasing $\gamma_1 L$ for both short-and long-term analyses (creep effects only), while, for a given $\gamma_1 L$, these tend to drop while decreasing $\gamma_2 L$. Despite these increases in the vertical deflection, the values calculated for the bottom slip, i.e., s_{z2}, tend to decrease due to slight movements of the neutral axis locations which occur due to the changes in cross-sectional properties; on the other hand, this change produces a slightly increase in the top slip, i.e., s_{z1}.

Even if the deflections due to shrinkage tend to decrease while reducing $\gamma_1 L$, the relative change in the results obtained using a 10 mm longitudinal plate are noted to increase when compared against those calculated with a 50 mm stiffening plate.

8.3. Effects of concrete strength

The influence of the concrete strength becomes more apparent when considering the time-dependent behaviour as outlined in Table 3. Reducing the concrete strength from 32 MPa to 25 MPa increases the instantaneous deflection by approx. 2% and the long-term one due to creep by up to 5.5%. Shrinkage deflections increase by a greater amount (up to nearly 9%) even if this is partly due to the fact that

Table 2 Variations (%) between the results obtained reducing the longitudinal plate thickness from 50 mm to 10 mm

Deflection at mid-span													
$\gamma_1 L$	$\gamma_2 L$	Instantaneous values at t_0				Values at time t (creep effects only)				Values at time t (shrinkage effects only)			
		L1	L2	L3	L4	L1	L2	L3	L4	L1	L2	L3	L4
100	100	0.00%	17.57%	36.46%	50.26%	0.00%	14.73%	29.48%	39.60%	3.22%	5.97%	8.39%	3.22%
	1	0.00%	0.08%	0.54%	2.60%	0.00%	0.08%	0.47%	2.28%	0.02%	0.13%	0.68%	0.02%
1	100	0.00%	11.60%	22.31%	29.20%	0.00%	11.68%	22.49%	29.47%	4.96%	8.85%	11.08%	4.96%
	1	0.00%	0.07%	0.42%	1.93%	0.00%	0.07%	0.42%	1.95%	0.04%	0.20%	0.91%	0.04%
Slip between the steel joist and the longitudinal plate (calculated at the extremes of the longitudinal plate)													
$\gamma_1 L$	$\gamma_2 L$	Instantaneous values at t_0				Values at time t (creep effects only)				Values at time t (shrinkage effects only)			
		L1	L2	L3	L4	L1	L2	L3	L4	L1	L2	L3	L4
100	100	n/a	-3.31%	-3.39%	-4.67%	n/a	-3.27%	-3.33%	-4.34%	n/a	-7.56%	-7.60%	-7.69%
	1	n/a	-1.49%	-1.54%	-1.77%	n/a	-1.84%	-1.88%	-2.06%	n/a	-6.08%	-6.12%	-6.27%
1	100	n/a	-3.08%	-3.17%	-3.31%	n/a	-2.95%	-3.03%	-3.10%	n/a	-6.26%	-6.34%	-6.41%
	1	n/a	-2.77%	-2.79%	-2.83%	n/a	-2.77%	-2.78%	-2.81%	n/a	-6.06%	-6.06%	-6.09%

NOTE: the variation (%) has been calculated specifying a concrete strength of 32 MPa, a relative humidity of 80% and reducing the longitudinal plate from 50 mm to 10 mm:
Variation(%) = [*solution*(with 10 mm)-*solution*(with 50 mm)]/*solution*(with 50 mm)

Table 3 Variations (%) between the results obtained reducing the concrete strength from 32 MPa to 25 MPa

Deflection at mid-span													
$\gamma_1 L$	$\gamma_2 L$	Instantaneous values at t_0				Values at time t (creep effects only)				Values at time t (shrinkage effects only)			
		L1	L2	L3	L4	L1	L2	L3	L4	L1	L2	L3	L4
100	100	1.56%	1.78%	2.01%	2.17%	4.42%	4.84%	5.25%	5.54%	5.48%	5.43%	5.38%	5.34%
	1	1.56%	1.57%	1.57%	1.59%	4.42%	4.42%	4.42%	4.44%	5.48%	5.48%	5.48%	5.46%
1	100	0.09%	0.08%	0.07%	0.07%	0.09%	0.08%	0.07%	0.07%	8.29%	8.29%	8.27%	8.26%
	1	0.09%	0.10%	0.10%	0.09%	0.09%	0.09%	0.09%	0.08%	8.29%	8.29%	8.29%	8.29%
Slip between the steel joist and the longitudinal plate (calculated at the extremes of the longitudinal plate)													
$\gamma_1 L$	$\gamma_2 L$	Instantaneous values at t_0				Values at time t (creep effects only)				Values at time t (shrinkage effects only)			
		L1	L2	L3	L4	L1	L2	L3	L4	L1	L2	L3	L4
100	100	n/a	0.37%	0.37%	0.34%	n/a	1.27%	1.27%	1.18%	n/a	5.51%	5.50%	6.32%
	1	n/a	0.40%	0.40%	0.40%	n/a	1.36%	1.36%	1.35%	n/a	5.58%	5.57%	5.60%
1	100	n/a	0.08%	0.07%	0.06%	n/a	0.06%	0.06%	0.05%	n/a	8.37%	8.39%	8.43%
	1	n/a	0.09%	0.09%	0.09%	n/a	0.07%	0.07%	0.07%	n/a	8.38%	8.39%	8.40%

NOTE: the variation (%) has been calculated specifying a 50 mm thick longitudinal plate, a relative humidity of 80% andreducing the concrete strength from 32 MPa to 25 MPa:
Variation(%) = [*solution*(with 25MPa)-*solution*(with 32MPa)]/*solution*(with 32MPa)

shrinkage induced strains increase while decreasing concrete strengths; similar considerations apply to the values of the bottom slip.

Table 4 Variations (%) between the results obtained reducing the relative humidity from 80% to 50%

Deflection at mid-span									
$\gamma_1 L$	$\gamma_2 L$	Values at time t (creep effects only)				Values at time t (shrinkage effects only)			
		L1	L2	L3	L4	L1	L2	L3	L4
100	100	7.75%	8.49%	9.21%	9.71%	71.12%	70.99%	70.86%	70.76%
	1	7.75%	7.76%	7.78%	7.86%	71.12%	71.12%	71.12%	71.08%
1	100	0.15%	0.14%	0.13%	0.12%	78.62%	78.60%	78.56%	78.55%
	1	0.15%	0.15%	0.14%	0.14%	78.62%	78.62%	78.62%	78.61%
Slip between the steel joist and the longitudinal plate (calculated at the extremes of the longitudinal plate)									
$\gamma_1 L$	$\gamma_2 L$	Values at time t (creep effects only)				Values at time t (shrinkage effects only)			
		L1	L2	L3	L4	L1	L2	L3	L4
100	100	n/a	2.22%	2.22%	2.07%	n/a	71.16%	71.14%	73.30%
	1	n/a	2.38%	2.38%	2.36%	n/a	71.35%	71.34%	71.41%
1	100	n/a	0.10%	0.10%	0.08%	n/a	78.81%	78.84%	78.97%
	1	n/a	0.12%	0.12%	0.12%	n/a	78.85%	78.86%	78.88%

NOTE: the variation (%) has been calculated specifying a 50 mm thick longitudinal plate, a concrete strength of 32 MPa and reducing the relative humidity from 80% to 50%:
Variation(%) = [*solution*(with 50%)-*solution*(with 80%)]/*solution*(with 80%)

8.4. Effects of relative humidity

The time-dependent behaviour of the concrete is highly affected by the relative humidity of the ambient. This is depicted in Table 4 where the results based on a relative humidity (RH) of 80% have been compared against those calculated using a RH of 50%. There is a significant increase in the long-term deflections accounting for both creep and shrinkage effects; nevertheless, this is mainly attributed to the different concrete behaviour at these different humidity levels. Looking at the general trend it can be noted that decreasing the relative humidity mainly affects the response for higher values of $\gamma_1 L$ leading to increased displacements.

Table 5 Variations (%) between the mid-span deflections calculated using the effective flexural rigidity determined following guidelines EC5 Annex B and those obtained based on the proposed finite element

Mid-span deflection calculated at time t_0							
$\gamma_1 L$	$\gamma_2 L$	Additional longitudinal plate: 450 mm×50 mm Concrete strength: 32MPa Relative humidity: 80%			Additional longitudinal plate: 450 mm×10 mm Concrete strength: 32MPa Relative humidity: 80%		
		EC5 – $v(L/2)$ in m	FEM – $v(L/2)$ in m	error	EC5 – $v(L/2)$ in m	FEM – $v(L/2)$ in m	error
100	100	0.01970	0.01970	-0.01%	0.02960	0.02959	-0.01%
	1	0.03327	0.03326	-0.02%	0.03413	0.03413	-0.01%
1	100	0.06311	0.06310	-0.02%	0.08154	0.08152	-0.02%
	1	0.08827	0.08824	-0.03%	0.08997	0.08995	-0.02%

NOTE: the error (%) has been calculated comparing the results obtained based on the flexural rigidity calculated in accordance with EC5 Annex B and those determined by means of the proposed finite element:
Error(%) = [*solution*(FEM)-*solution*(EC5)]/*solution*(FEM)

8.5. Comparisons with results obtained by means of EC5 Annex B

The accuracy of available design guidelines EC5 (1995) dealing with the behaviour of multilayered beams with flexible shear connection have been evaluated. EC5 (1995) provides an expression to determine the effective flexural rigidity of a multi-layered member with flexible connection which has been utilized to calculate the mid-span deflection based on full interaction theory considering the 25 m simply supported beam utilised in the previous parametric study with stiffening arrangement A4. Table 5 highlights the adequacy of the EC5 approach which yields an error less than 1% for all combinations of shear connection stiffness (Table 1) and for different thicknesses of the longitudinal plate.

9. Conclusions

This paper described a novel analytical model for the analysis of three-layered beams with partial shear interaction. In particular, the analytical formulation has been outlined considering the case of a composite beam stiffened by means of a longitudinal plate bolted to the bottom flange of the steel joist. The analytical model has been derived using the principle of virtual work relying on a specified displacement field. For numerical applications, a novel finite element with 13 degree-of-freedom has been derived, whose nodal freedoms include the axial displacements of each layer, the vertical displacements and the rotations at each element ends. The accuracy of this element has been validated against known short-and long-term solutions with full shear interaction, assuming that both shear connection stiffnesses tend to infinity, and with partial shear interaction of only two layers, in which case only one shear connection is assumed to be infinitively stiff.

A parametric study has been carried out to investigate the influence on the short-and long-term behaviour of the composite beam of the shear connection stiffness between the concrete slab and the steel joist, the stiffness of the plate-to-beam connection, the properties of the longitudinal plate and the concrete properties. For this purpose, four different stiffening arrangements using an additional longitudinal plate have been considered. The proposed numerical examples have highlighted the general applicability of the proposed approach and its ease of use in determining the structural response at service level for different retrofitting solutions.

The accuracy of EC5 guidelines to depict the behaviour of elastic multi-layered beams with flexible shear connection has been validated and it has been shown that for the cross-sectional properties considered the calculation of the mid-span deflections for a simply supported structural system remains within a negligible error, i.e., less than 1%, when compared to the finite element solutions. For this purpose, the effective flexural rigidity calculated in accordance with EC5 guidelines was utilised to determine the deflection based on full interaction theory. These comparisons have been carried out for different combinations of the two shear connection stiffnesses.

References

Amadio, C. and Fragiacomo, M. (2005), "Effective width evaluation of steel-concrete composite beams", *J. Const. Steel Res.*, **58**, 373-388.

Ayoub, A. (2001), "A two-field mixed variational principle for partially connected composite beams", *Finite*

Elements in Analysis and Design, **37**, 929-959.
Ayoub, A. and Filippou, F. C. (2000), "Mixed formulation of nonlinear steel-concrete composite beam element", *J. Struct. Eng.*, ASCE, **126**(3), 371-381.
Bažant, Z. P. (1972), "Prediction of concrete creep effects using age-adjusted effective modulus method", *ACI J.*, **69**(4), 212-217.
Bažant, Z. P. and Oh, B. H. (1984), "Deformation of progressively cracking reinforced concrete beams", *ACI J.*, **81**(3), 268-278.
Čas, B., Bratina, S., Saje, M. and Planinc, I. (2004), "Non-linear analysis of composite steel-concrete beams with incomplete interaction", *Steel and Composite Structures*, **4**(6), 489-507.
CEB (Comité Euro-International du Béton), (1984) *CEB Design Manual on Structural Effects of Time-Dependent Behaviour of Concrete*, edited by Chiorino, M. A., Napoli, P., Mola, F. and Koprna, M., Georgi Publishing, Saint-Saphorin, Switzerland.
CEB-FIB (Comité Euro-International du Béton -Fédération International de la Précontrainte) (1993), *Model Code 1990: Design Code,* Thomas Telford, London.
Cook, R., Malkus, D., Plesha, M. and Witt, R. (2001), *Concepts and Applications of Finite Element Analysis*, 4th edition, Wiley.
Cosenza, E. and Mazzolani, S. (1993), "Linear-elastic analysis of composite beams with partial shear interaction", *Proc. of the First Italian Workshop on Composite Structures*, University of Trento June 1993. (In Italian)
Cosenza, E. and Zandonini, R. (1999), "Composite Construction", edited by Chen Wai-Fah in *Structural Engineering Handbook*, CRC Press LLC.
Dall'Asta, A. and Zona, A. (2004), "Three-field mixed formulation for the non-linear analysis of composite beams with deformable shear connection", *Finite Elements in Analysis and Design*, **40**, 425-448.
Dall'Asta, A. and Zona, A. (2002), "Non-linear analysis of composite beams by a displacement approach", *Comp. Struct.*, **80**, 2217-2228.
Dezi, L., Gara, F., Leoni, G. and Tarantino, A. M. (2001), "Time dependent analysis of shear-lag effect in composite beams", *J. Eng. Mech.*, **127**(1), 71-79.
Dezi, L., Leoni, G. and Tarantino, A. M. (1998), "Creep and shrinkage analysis of composite beams", *Progress in Structural Engineering and Materials*, **1**(2), 170-177.
Dezi, L., Leoni, G. and Tarantino, A. M. (1996), "Algebraic methods for creep analysis of continuous composite beams", *J. Struct. Eng.,* ASCE, **122**(4), 423-430.
Dezi, L. and Tarantino, A. M. (1993a), "Creep in composite continuous beams - I: Theoretical treatment", *J. Struct. Eng.,* ASCE, **119**(7), 2095-2111.
Dezi, L. and Tarantino, A. M. (1993b), "Creep in composite continuous beams - II: Parametric study", *J. Struct. Eng.,* ASCE, **119**(7), 2112-2133.
Eurocode 5 (1995), *Design of timber structures - Part 1.1: General rules and rules for buildings*, CEN.
Fabbrocino, G., Manfredi, G. and Cosenza, E. (2000), "Analysis of continuous composite beams including partial interaction and bond", *J. Struct. Eng.*, ASCE, **126**(11), 1288-1294.
Faella, C., Martinelli, E. and Nigro, E. (2003), "Steel connection nonlinearity and deflections of steel-concrete composite beams: A simplified approach", *J. Struct. Eng.*, ASCE, **129**(1), 12-20.
Faella, C., Martinelli, E. and Nigro, E. (2002), "Steel and concrete composite beams with flexible shear connection: "exact" analytical expression of the stiffness matrix and applications", *Comput. Struct.*, **80**, 1001-1009.
Fragiacomo, M., Amadio, C. and Macorini, L. (2002), "Influence of viscous phenomena on steel-concrete composite beams with normal or high performance slab", *Steel and Composite Structures*, **2**(2), 85-98.
Gattesco, N. (1999), "Analytical modelling of nonlinear behaviour of composite beams with deformable connection", *J. Constr. Steel Res.*, **52**, 195-218.
Gere, J. M. (2001), *Mechanics of Materials*, 5th edition, Brooks/Cole.
Gilbert, R. I. (1988), *Time Effects in Concrete Structures*, Elservier Science Publishers, Amsterdam, The Netherlands.
Gilbert, R. I. and Bradford, M. A. (1995), "Time-dependent behavior of continuous composite beams at service loads", *J. Struct. Eng.*, ASCE, **121**(2), 319-327.
Girhammar, U. A. and Pan, D. (1993), "Dynamic analysis of composite members with interlayer slip", *Int. J. Solids Struct.*, **30**(6), 797-823.
Goodman, J. R. and Popov, E. P. (1968), "Layered beam systems with interlayer slip", *J. Struct. Div., Proc. of*

the American Society of Civil Engineers, **94**(11), 2535-2547.
Kwak, H. G. and Seo, Y. L. (2002), "Time-dependent behaviour of composite beams with flexible connectors", *Comput. Method Appl. Mech. Eng.*, **191**, 3751-3772.
Loh, H., Uy, B. and Bradford, M. A. (2004), "The effects of partial shear interaction in the hogging moment regions of composite beams: Part II - Analytical study", *J. Constr. Steel Res.*, **60**, 921-962.
Moin, P. (2001), *Fundamentals of Engineering Numerical Analysis*, Cambridge University Press.
Newmark, N. M., Siess, C. P. and Viest I. M. (1951), "Tests and analysis of composite beams with incomplete interaction", *Proc. of the Society of Experimental Stress Analysis*, **9**(1), 75-92.
Nguyen, N. T., Oehlers, D. J. and Bradford, M. A. (1998), "A rational model for the degree of interaction in composite beams with flexible shear connectors", *Mechanics of Structures and Machines*, **26**(2), 175-194.
Oehlers, D. J. and Bradford, M. A. (1995), *Composite Steel and Concrete Structural Members: Fundamental Behaviour*, Pergamon Press, Oxford.
Oehlers, D. J. and Sved, G. (1995), "Composite beams with limited-slip-capacity connectors", *J. Struct. Eng.*, ASCE, **121**(6), 932-938.
Ranzi, G. and Bradford, M. A. (2006), "Analytical solutions for the time-dependent behaviour of composite beams with partial interaction", *Int. J. Solids Struct.*, **43**(13), 3770-3793.
Ranzi, G. and Bradford, M. A. (2005), "Time analysis of structural concrete elements using the equivalent displacement approach", *Mater. Struct.*, **38**(280), 609-616.
Ranzi, G., Bradford, M. A. and Uy, B. (2004), "A direct stiffness analysis of a composite beam with partial interaction", *Int. J. Numer. Methods Eng.*, **61**, 657-672.
Salari, M. R. and Spacone, E. (2001), "Finite element formulations of one-dimensional elements with bond-slip", *Eng. Struct.*, **23**(7), 815-826.
Seracino, R., Lee, C. T., Lim, T. C. and Lim, J. Y. (2004), "Partial interaction stresses in continuous composite beams under serviceability loads", *J. Constr. Steel Res.*, **60**, 1525-1543.
Tarantino, A. M. and Dezi, L. (1992), "Creep effects in composite beams with flexible shear connectors", *J. Struct. Eng.*, ASCE, **118**(8), 2063-2081.
Virtuoso, F. and Vieira, R. (2004), "Time dependent behaviour of continuous composite beams with flexible connection", *J. Constr. Steel Res.*, **60**, 451-463.
Wu, Y. F., Oehlers, D. J. and Griffith, M. C. (2002), "Partial-interaction analysis of composite beam/ column members", *Mech. Struct. Mach.*, **30**(3), 309-332.

Appendix

$$A\tilde{E}_1 = \int_{A_c} \Delta_{1k}\, \mathrm{d}a + \int_{A_r} E_r\, \mathrm{d}a; \qquad A\tilde{E}_2 = \int_{A_s} E_s\, \mathrm{d}a\ ; \qquad A\tilde{E}_3 = \int_{A_p} E_p\, \mathrm{d}a$$

$$B\tilde{E}_1 = \int_{A_c} \Delta_{1k}(y - y_1)\, \mathrm{d}a + \int_{A_r} E_r(y - y_1)\, \mathrm{d}a\ ; \qquad B\tilde{E}_2 = \int_{A_s} E_s(y - y_2)\, \mathrm{d}a\ ; \qquad B\tilde{E}_3 = \int_{A_p} E_p(y - y_3)\, \mathrm{d}a$$

$$I\tilde{E}_1 = \int_{A_c} \Delta_{1k}(y - y_1)^2\, \mathrm{d}a + \int_{A_r} E_r(y - y_1)^2\, \mathrm{d}a\ ; \qquad I\tilde{E}_2 = \int_{A_s} E_s(y - y_2)^2\, \mathrm{d}a\ ; \qquad I\tilde{E}_3 = \int_{A_p} E_p(y - y_3)^2\, \mathrm{d}a$$

$$\mathbf{T}=\begin{bmatrix} A\tilde{E}_1 & 0 & 0 & 0 & 0 & 0 & B\tilde{E}_1 & 0 \\ & A\tilde{E}_2 & 0 & 0 & 0 & 0 & B\tilde{E}_2 & 0 \\ & & A\tilde{E}_3 & 0 & 0 & 0 & B\tilde{E}_3 & 0 \\ & & & k_{z1} & -k_{z1} & 0 & 0 & k_{z1}h_1 \\ & & & & k_{z1}+k_{z2} & -k_{z2} & 0 & k_{z2}h_2-k_{z1}h_1 \\ & & & & & k_{z2} & 0 & -k_{z2}h_2 \\ & sym & & & & & \sum_{i=1}^{3} I\tilde{E}_i & 0 \\ & & & & & & & k_{z1}h_1^2+k_{z2}h_2^2 \end{bmatrix}; \qquad \partial \equiv \frac{\mathrm{d}}{\mathrm{d}\,z}$$

$$\mathscr{A}^{\mathrm{T}}=\begin{bmatrix} \partial & 0 & 0 & 1 & 0 & 0 & 0 & 0 \\ 0 & \partial & 0 & 0 & 1 & 0 & 0 & 0 \\ 0 & 0 & \partial & 0 & 0 & 1 & 0 & 0 \\ 0 & 0 & 0 & 0 & 0 & 0 & -\partial^2 & -\partial \end{bmatrix}; \qquad \mathscr{B}^{\mathrm{T}}=\begin{bmatrix} 1 & 0 & 0 & 0 & 0 \\ 0 & 1 & 0 & 0 & 0 \\ 0 & 0 & 1 & 0 & 0 \\ 0 & 0 & 0 & 1 & -\partial \end{bmatrix}$$

$$\Delta_{1k}=\frac{2}{J(t_k,t_k)+J(t_k,t_{k-1})}; \qquad \Delta_{2ki}=\begin{cases} \dfrac{J(t_k,t_1)-J(t_k,t_0)}{J(t_k,t_k)+J(t_k,t_{k-1})} & \text{for } i=0 \\ \dfrac{J(t_k,t_{i+1})-J(t_k,t_{i-1})}{J(t_k,t_k)+J(t_k,t_{k-1})} & \text{for } i=1,\ldots,k-1 \end{cases}$$

CC